J. Membrane Biol. 170, 121–133 (1999)

The Journal of
Membrane
Biology

Resistivity of Red Blood Cells Against High-Intensity, Short-Duration Electric Field Pulses Induced by Chelating Agents

H. Mussauer[1], V.L. Sukhorukov[1], A. Haase[2], U. Zimmermann[1]
Lehrstuhl für Biotechnologie, Biozentrum,[1] and Lehrstuhl für Experimentelle Physik (Biophysik),[2] Universität Würzburg, Am Hubland, D-97074 Würzburg, Germany

Received: 19 January 1999/Revised: 1 April 1999

Abstract. The interaction of human red blood cells (RBCs) with diethylenetriamine-pentaacetic acid (DTPA) or its Gd-complex (Magnevist, a widely used clinical magnetic resonance contrast agent containing free DTPA ligands) led to the following, obviously interrelated phenomena. (i) Both compounds protected erythrocytes against electrohemolysis in isotonic solutions caused by a high-intensity DC electric field pulse. (ii) The inhibition of electrohemolysis was observed only when cells were electropulsed in low-conductivity solutions. (iii) The uptake of Gd-DTPA by electropulsed RBCs was relatively low. (iv) (Gd-) DTPA reduced markedly deformability of erythrocytes, as revealed by the electrodeformation experiments using high-frequency electric fields. Taken together, the results indicate that (Gd-) DTPA produce stiffer erythrocytes that are more resistant to electric field exposure. The observed effects of the chelating agents on the mechanical properties and the electropermeabilization of RBCs must have an origin in molecular changes of the bilayer or membrane-coupled cytoskeleton, which, in turn, appear to result from an alteration of the ionic equilibrium (e.g., Ca^{2+} sequestration) in the vicinity of the cell membrane.

Key words: Erythrocytes — Deformability — DTPA — Electropermeabilization — Electrodeformation — Electrorotation

Introduction

Chelation of the Gd^{3+} ions with diethylenetriamine-pentaacetic acid (DTPA), an EDTA derivative, results in a stable, strongly paramagnetic complex that is widely used as a magnetic resonance (MR) contrast agent for diagnostic purposes. After intravenous administration, Gd-DTPA (Magnevist) and other conventional low-molecular-weight MR contrast agents pass rapidly out of the intravascular space and equilibrate with the surrounding tissues prior to renal excretion. The extremely hydrophilic Gd-DTPA does not permeate plasma membranes of cells and serves, therefore, as an efficient marker of the extracellular water and the blood-brain barrier function. However, due to its short intravascular residence time and unfavorable MR-contrast distribution, Gd-DTPA is less useful for tissue perfusion and microvessel studies [4, 12].

The ultimate aim of the present study is the production of a strictly intravascular (blood pool) MR contrast agent by loading red blood cells (RBCs) with Gd-DTPA. This should not only increase the time interval available for MR angiography after contrast agent injection but also reduce the undesirable paramagnetic doping of the nonvascular space. Other blood pool contrast agents where the paramagnetic moiety is linked to macromolecules, e.g., Gd-DTPA-polylysine, -dextran, -albumin [40], have certain limitations such as immunogenecity, trapping by the liver and spleen, etc. In contrast, autologous RBCs or lymphocytes bearing a paramagneticum would be an ideal blood pool MR contrast agent because of their perfect biocompatibility.

A promising approach for the introduction of Gd-chelates into living cells is electropermeabilization [for review *see* 30, 51]. This field technique has gained wide acceptance as the most reliable and reproducible single-step method of loading normally impermeant xenomolecules such as drugs, proteins, plasmids etc., into the cell interior [13, 49]. Electropermeabilization is based on the reversible electric breakdown of cell membranes, that

Correspondence to: U. Zimmermann

occurs when the induced transmembrane potential exceeds 1 *V* (at room temperature). A single (or a train of) high-intensity, short-duration electric field pulse(s) is required to induce reversible breakdown of the plasma membrane that causes a temporal loss of membrane impermeability. Such field-treated cells restore their original membrane integrity (reseal) within minutes or hours depending on the temperature. Besides the field pulse parameters (intensity, duration), the degree of electropermeabilization and, therefore, the quantity of the entrapped (or released) compound is strongly influenced by the pulse medium composition (Ca^{2+}, EDTA) [50] and conductivity [9, 43].

In this study we found that human RBCs electropulsed in Magnevist-containing media tolerated higher field strengths than control cells did. The strong protective effect of Magnevist against electrohemolysis was most likely due to the presence of free DTPA ligands, whose excess in Magnevist solution is necessary to guarantee complete coordination of the highly toxic free Gd^{3+} ions [12, 15]. We also found that the deformability of erythrocytes treated with (Gd-) DTPA (without electropulsing) decreased markedly whereas their electrical properties remained unchanged, as revealed by the electrodeformation and electrorotation experiments using high-frequency linear and rotating electric fields. The results presented here indicate that treatment with chelating agents stiffens erythrocytes, which, in turn, renders these cells more resistant to electric field exposure.

Materials and Methods

Cells

Blood samples (3–5 drops) were withdrawn from apparently healthy male donors and suspended in 10 mL DPBS (Dulbecco's phosphate buffered saline containing (in mM): 137 NaCl, 2.7 KCl, 1.5 KH_2PO_4, 8.1 Na_2HPO_4, pH 6.6 *see* below). The red blood cells (RBCs) were washed with DPBS and pelleted by centrifugation (10 min, 650 × *g*). The cells were kept in DPBS at 4°C and used on the day of collection.

Chemicals and Electromanipulation Media

Stock solutions of inositol (Sigma, I-5125), KCl (analytical grade, Sigma) and diethylenetriamine-N,N,N′,N″,N″-pentaacetic acid (DTPA, Sigma, D-6518) were prepared in double distilled water. Gd-DTPA (Magnevist) was purchased from Schering AG (Berlin, Germany). The osmolality of all stock solutions was adjusted to 280–300 mOsm. All solutions contained 1.15 mM phosphate buffer (K_2HPO_4/KH_2PO_4) and 100 μM $CaCl_2$ to stabilize the cell membrane [24, 50]. To reduce cell crenation, a pH of 6.6 was used in all experiments [18].

For electropermeabilization and dielectric measurements, the stock solutions of inositol, of KCl and DTPA (or Magnevist) were mixed to produce the desired conductivity and concentration of DTPA (or Magnevist). Conductivity and osmolality of the solutions were measured by means of a conductometer (Knick GmbH, Berlin, Germany) and a cryoscope (Osmomat 030, Gonotec GmbH, Berlin, Germany).

Electropermeabilization of Cells

Electrohemolysis

Ten minutes before electropermeabilization, the cells were transferred into isotonic pulse media of different compositions and conductivities. The final density was 2–3 × 10^6 cells per ml. The cells were subjected to a single exponentially decaying pulse of 4 kV/cm strength and a decay time constant of 20 μsec (at 22–24°C) by using a commercial electroporator (Biojet MI, Biomed, Theres, Germany). The discharge chamber (volume 1.1 ml) consisted of two flat stainless-steel electrodes (0.6 cm apart). As an indicator of the electropermeabilization process the field-induced hemoglobin (Hb) release from the cells was used. Ten minutes after field application, the samples were centrifuged (650 × *g*, 10 min), and the absorbance spectra of the supernatants in the wavelength range from 350 to 700 nm were measured by using a Perkin-Elmer Lambda 2 UV/VIS spectrophotometer (Überlinger, Germany). The 415 nm absorbance of the samples was used to quantitate Hb in the supernatants. Absorbance values for 100% Hb release were obtained by the addition of saponin (0.2%; Merck No. 7695).

Electroinjection of Gd-DTPA

The mean amount of Gd per cell taken up by the erythrocytes electropulsed in the presence of Magnevist was determined as follows. Ten minutes before field exposure, RBCs (10^8 cells/ml) were suspended in pulse media containing 20 mM Magnevist. Conductivity of the pulse media was 1.3–1.4 mS/cm at 22°C. The cells were then subjected to one electrical pulse of various intensities from 2 to 7 kV/cm (duration 20 or 40 μsec) at 4°C or at 22°C. After electrical treatment the cells were kept at 4°C (or 22°C) for the following 10 min and then transferred into a centrifuge tube containing 10 ml DPBS at room temperature. The cells were incubated for 15 min in this solution, then washed three times with 10 ml DPBS (400 × *g*, 10 min). About 10 μl of the peletted (packed) erythrocytes was diluted in 250 μl of DPBS, and 10 μl of this suspension was used for cell counting and volume determination by means of an electronic cell counter CASY1 (Schärfe System, Reutlingen, Germany). The remaining cells were lysed with 6% nitric acid, and Gd concentration in these samples was determined using an inductively coupled plasma emission spectroscope (ICP-OES, JY 70 Plus, Jobin Yvon, France).

Electrodeformation and Electrorotation

A computer-controlled pulse generator HP 8130A (Hewlett-Packard, Boeblingen, Germany) was used to feed the electrodes of two different microchambers which were used for electrodeformation and electrorotation measurements. The deformation chamber consisted of a planar array of 20 parallel interdigitated microelectrodes. The electrode fingers (made of platinum) were 0.5 μm thick, 33 μm wide and 1 mm long. The gap between neighboring electrodes was 46 μm. Electrorotation spectra were measured in a microstructured four-electrode chamber, which was arranged as a planar array of circular electrodes (made of gold) of 60 μm diameter, 1 μm thickness and 300 μm electrode spacing. Both microstructures were kindly supplied by G. Fuhr (Humboldt University, Berlin) [14, 18]. The adjacent electrodes of the chambers were driven with two 180° phase shifted (deformation) or four 90° phase shifted (rotation) rectangular signals from the pulse generator with frequencies from 1 kHz up to 300 MHz for AC and up to 150 MHz

for rotating fields. The electrodeformation and rotation responses of RBCs were observed by using a microscope (BX50, Olympus, Hamburg, Germany) equipped with a CCD camera (SSC-M370CE, Sony, Cologne, Germany). The video camera was connected to a monitor and to a personal computer equipped with a video digitizing board and an image capture software "Screen Machine II" (Fast Electronics, Munich, Germany).

Typically, 50 μl of cell suspension (1–3 × 10^5 cells/ml) was pipetted into the microchambers and a coverslip was gently placed over it. For electrodeformation measurements, cells were given to settle for about 1 min, and a 40 MHz field of 0.4 kV/cm was then applied for 5–10 sec to direct cells to the electrode edges by positive dielectrophoresis. In contrast, electrorotation measurements were performed only on lone cells near the center of the four-electrode chamber. The electrodeformation and rotation spectra were monitored by decreasing the field frequency in steps (5–10 points per decade of frequency starting at 250 MHz) while the field strength was kept constant. In electrorotation experiments, 1 to 4 revolutions of the cell were timed with a stopwatch at each field frequency. The electrodeformation spectra, that is the relative deformation [strain = $(l - l_0)/l_0$] as a function of field frequency, were evaluated from the sequences of about 20 images of the same cell sample (usually 10–12 cells). The field strength dependence of the deformation was measured at a frequency of 10 MHz by increasing the applied voltage from 0 to 9.6 V_{PP} (0–2.1 kV/cm) in 1*V* steps. For each erythrocyte, its maximal original length (l_0, without field) and its maximal length (l, after field application) in the direction parallel to the field lines at various frequencies (or strengths) were determined using a commercial image measurement software "SigmaScan" (Jandel GmbH, Erkrath, Germany). The rotation and deformation spectra were fitted on the basis of the single-shell model using the *Mathematica* software. The spectra were corrected by the scaling factors, χ ($= \varepsilon_\varepsilon \cdot \varepsilon_0 \cdot E^2/2\eta$) and α (*see* Appendix), that account for the local field strength and frictional force experienced by an individual cell (rotation), and for the elastic cell properties (deformation), respectively.

Results

Effect of DTPA and Magnevist on Electropermeabilization

Electrohemolysis

Human RBCs were exposed to one electric pulse of 4 kV/cm (duration 20 μsec) in media of the same conductivity but containing various concentrations of DTPA or Gd-DTPA. The field strength of 4 kV/cm is nearly twice as high as the critical intensity required to reach the breakdown voltage at membrane sites located in field direction (assuming an average cell radius of 3–4 μm; *see* [50]. To exclude the conductivity effect on electrohemolysis, the conductivity of all pulse media used in this experiment was adjusted to the same value of 2.4–2.7 mS/cm. The percentage of electrohemolysis was used to quantitate membrane permeabilization. In control experiments, DTPA- (Magnevist-) free pulse media containing KCl were used.

Figure 1 shows the effects of increasing concentrations of DTPA and Magnevist on electrohemolysis. The

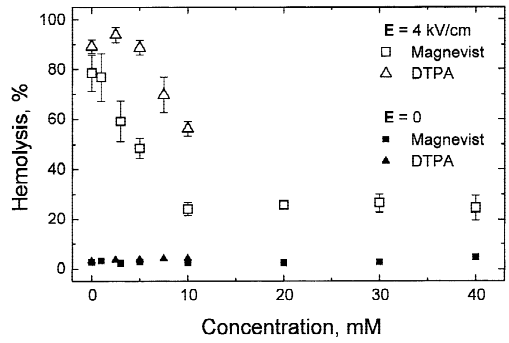

Fig. 1. Dependence of the electrohemolysis of human erythrocytes (in percentage) on the concentration of DTPA (open triangles) and Gd-DTPA (Magnevist, open squares). The cells were exposed at 22–24°C to one electrical pulse (20 μsec) of 4 kV/cm in isotonic media (280 mosmol/kg). The conductivity of the pulse media containing 0–40 mM Magnevist or 0–10 mM DTPA was adjusted to 2.4–2.7 mS/cm by addition of appropriate amounts of KCl. The released hemoglobin was determined spectrophotometrically in the supernatants 10 min after field application. The electrohemolysis decreased significantly when the concentrations of Magnevist and DTPA were equal (or greater) 3 mM ($P < 0.02$) and 7.5 mM ($P < 0.05$), respectively. The hemolysis without field treatment did not exceed 3–5% (solid symbols). The data points are the means of 3–4 independent measurements; the bars represent the standard error (SE).

addition of 1 mM Magnevist or 2.5–5 mM DTPA had no effect on electrohemolysis, i.e., the percentage of electrohemolysis in these samples (78–94%) was similar to that observed in control cells (78–90%). The increase of Magnevist concentration in pulse medium from 1 to 20 mM reduced gradually the degree of electrohemolysis from 78% to a minimum value of 24%. The percentage of electrohemolysis in more concentrated Magnevist solutions (20–40 mM) remained unchanged (24–26%). The effect of DTPA on electrohemolysis was similar to that of Magnevist. Thus, the increase of DTPA concentration from 5 to 10 mM caused a decrease of electrohemolysis from 90 to about 55%. Measurements at DTPA concentrations greater than 10 mM were not performed because conductivity of such solutions exceeds the value of 2.4–2.7 mS/cm (*see above*).

As already mentioned, the degree of electropermeabilization of mammalian cells depends sensitively on the conductivity of the suspending medium. Therefore, the effect of Magnevist on electrohemolysis was studied using electromanipulation media of various conductivities (but of the same tonicity and Gd-DTPA concentration, Fig. 2). At high, nearly physiological conductivities, i.e., at $\sigma_e > 5$ mS/cm, the electrohemolysis was negligible (5–9%) in both control and Magnevist treated RBC samples (Fig. 2, open circles and squares, respectively). For control cells, the electrohemolysis grew markedly from 9% (5 mS/cm) to 96% (2 mS/cm) with decreasing conductivity. By contrast, the decrease of conductivity from 5 to 2 mS/cm caused only a slight rise

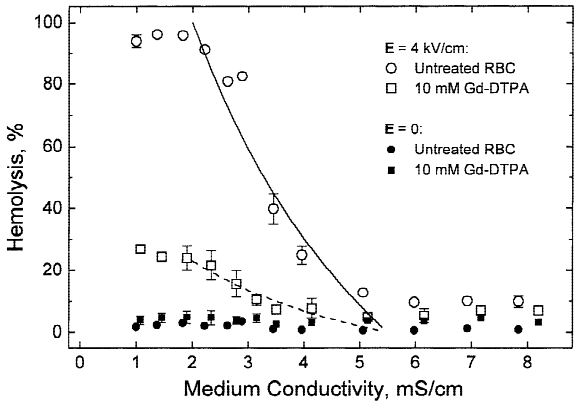

Fig. 2. Effect of Magnevist (10 mM) on the electrohemolysis of human RBCs exposed at 22–24°C to one electrical pulse (20 μsec) of 4 kV/cm in isotonic media of various conductivities. At conductivities higher than 5 mS/cm, the electrohemolysis was negligible (less than 10%). In Magnevist-free pulse media (open circles), the electrohemolysis grew rapidly with decreasing conductivity and achieves 95–98% at about 2 mS/cm. In the presence of Magnevist (open squares), the cells become much more resistant to electropulsing, i.e., the maximum value of electrohemolysis was 27% at the lowest conductivity of 1 mS/cm. The solid symbols represent the hemolysis data of cells without electric field exposure. The curves show the theoretical relationship between the cytosolic polarization of the cell $U_{int} = (\sigma_i - \sigma_e)/(\sigma_i + 2\sigma_e)$ (*see* Table) and the medium conductivity, σ_e (the curves are normalized to the data points obtained at $\sigma_e = 2$ mS/cm. For further explanation, *see* Appendix).

of Hb-release from 5 to 24% if 10 mM Magnevist had been added to the pulse medium. It is clearly seen, that although the conductivity dependence of the electrohemolysis in Magnevist-treated cell samples is qualitatively similar to that of control cells, Magnevist suppresses the electrohemolysis in the 1–2 mS/cm conductivity range by a factor of 3–4. The hemolysis without field exposure was negligible (less than 5%) in both control and Magnevist (or DTPA) treated cell samples (Figs. 1 and 2, solid symbols). The results shown in Figs. 1 and 2 suggest that both Magnevist and DTPA increase markedly the resistivity of human RBCs against electric field pulses.

Electro-uptake of Gd-DTPA

The mean intracellular concentration of Gd (Gd_i) in the erythrocytes electropulsed in the presence of 20 mM Magnevist was determined by means of the atomic emission spectroscopy. In this series of experiments, RBC samples were exposed to one electric pulse of 20–40 μsec duration at 20°C or at 4°C. The field strength was varied from 2 to 7 kV/cm in steps of 1 kV/cm. At room temperature, the maximum Gd_i value of about 100 μM in a mean surviving cell was obtained after treatment with an electric pulse of 3 kV/cm intensity and 40 μsec duration. The percentage of surviving cells in this experiment was about 50%, as revealed by cell counting 30 min after field exposure. At 4°C, stronger electric fields had to be used to achieve detectable loading of RBCs with Gd-DTPA, e.g., a somewhat higher Gd_i (≈ 150 μM) concentration was obtained with a pulse of 7 kV/cm strength and 40 μsec duration, albeit at the expense of cell viability (85% cell loss). The observation that the influx of Gd-DTPA into electropulsed erythrocytes was relatively low is consistent with our finding that (Gd-) DTPA protects RBCs against electropermeabilization (*see* the Hb-efflux data shown in Figs. 1 and 2).

Possible Mechanisms of Increased Electroresistivity of RBCs

There are at least three plausible explanations for the (Gd-) DTPA mediated resistivity of erythrocytes to electric field exposure and for the low electrouptake of Gd-DTPA:

(i) Shape and related size transformations of erythrocytes. Thus, it is well known that RBCs may undergo dramatic shape changes within minutes when chemical composition of the suspending medium is changed [16, 19]. A possible decrease of cell radius would reduce the induced membrane voltage and, therefore, suppress the electrosensitivity of erythrocytes ($V_g = 1.5 \cdot a \cdot E \cdot \cos \alpha$, *see* Appendix). This is also because cell size dependence is an important factor determining what proportion of the cell surface will be permeabilized by a pulse of given field strength.

(ii) Changes in the electrical properties of the plasma membrane and cytosol. Thus, the diffusion-driven ion loss from the cytosol of erythrocytes suspended in low-conductive media would decrease the internal conductivity σ_i, which in turn will affect the electrosensitivity of RBCs, e.g., via slower rate of membrane charging τ_m and reduced electrodeformation force F_{DEF} (Table) [43].

(iii) Alteration of cell deformability. It is well known that mechanical stability of RBCs is closely related to their deformability, which is very sensitive to various physicochemical factors, such as drugs, medium composition, cytosolic calcium concentration etc. [33, 34, 38]. Thus, treatment with several classes of chemicals has been reported not only to affect red cell deformability but also to protect these cells against freeze-thaw and osmotic stresses [3, 29].

To distinguish between these three possibilities, the following experiments were carried out: (i) measurements of cell size transformations by means of an electronic cell counter system; (ii) measurements of the mechanical and (iii) electrical properties of RBCs by means of the electrodeformation and electrorotation techniques, which employ high frequency, linear and rotating electric fields, respectively.

Table. Summary of some parameters important for the electropermeabilization and electromechanical responses of cells

Time scale; frequency range	Relaxation times; characteristic frequencies	Cell polarizability, U^* (Clausius-Mosotti function)	V_g (time); V_g (frequency)	Time constants§; characteristic frequencies		Re (U^*)§; Deformation	
		$U^* = \frac{\varepsilon_C^* - \varepsilon_e^*}{\varepsilon_C^* + 2\varepsilon_e^*}$	$1.5 \cdot a \cdot E \cdot (1 - \exp(-t/\tau_m))$ $1.5 \cdot a \cdot E \cdot (1 + (2\pi f \tau_m)^2)^{-0.5}$	$\sigma_e < \sigma_i$	$\sigma_e = \sigma_i$	$\sigma_e < \sigma_i$	$\sigma_e = \sigma_i$
$t < \tau_i$ $f > f_{c2}$		$U_h = \frac{\varepsilon_i - \varepsilon_e}{\varepsilon_i + 2\varepsilon_e}$	~0	<<2.8 nsec >58 MHz	<<1 nsec >150 MHz	−0.04	−0.04
$t \approx \tau_i$ $f \approx f_{c2}$	$\tau_i = \frac{1}{2\pi f_{c2}} = \frac{\varepsilon_i + 2\varepsilon_e}{\sigma_i + 2\sigma_e}$		~0	2.8 nsec 58 MHz	1 nsec 150 MHz		
$\tau_i < t < \tau_m$ $f_{c1} < f < f_{c2}$		$U_{int} = \frac{\sigma_i - \sigma_e}{\sigma_i + 2\sigma_e}$	~0	16 nsec 10 MHz	16 nsec 10 MHz	+0.57	−0.01
$t \approx \tau_m$ $f \approx f_{c1}$	$\tau_m = \frac{1}{2\pi f_{c1}} = aC_m\left(\frac{1}{\sigma_i} + \frac{1}{2\sigma_e}\right)$		↑	0.23 μsec 0.7 MHz	0.1 μsec 1.6 MHz		
$t > \tau_m$ $f < f_{c1}$		$U_1 = \frac{a \cdot G_m - \sigma_e}{a \cdot G_m + 2\sigma_e}$	$V_g = 1.5 \cdot a \cdot E$	>>0.23 μsec <0.7 MHz	>>0.1 μsec <1.6 MHz	−0.50	−0.50

The complex permittivities of homogeneous dielectrics and cells are given by $\varepsilon^* = \varepsilon - j \cdot \sigma/(2\pi f)$ and $\varepsilon_C^* = aC_m^*\varepsilon_i^*/(aC_m^* + \varepsilon_i^*)$, respectively. § The numeric values were calculated for two external conductivities σ_e of 1 and 5 mS/cm using the cell parameters given in the legend to Fig. A1.

Effects of DTPA and Magnevist on Cell Size

Measurements of the cell size were performed 10–20 min after the erythrocytes (about 20 μl) had been suspended in 10 ml of one of the three media at room temperature: (i) control (KCl-inositol), (ii) 10 mM Magnevist, and (iii) 5 mM DTPA. Conductivity and osmolality of these solutions had been adjusted to 1.23 mS/cm and 286–291 mOsm, respectively. The mean radii for about 2×10^3 cells were evaluated automatically from electronic size histograms by using a single-particle analyzer (*data not shown*).

We found that the mean "electronic" radius, *a*, for control cells was 3.1–3.15 μm. The erythrocytes treated with Magnevist or DTPA were somewhat larger: a = 3.25–3.35 μm and a = 3.15–3.2 μm, respectively. This means that changes in the cell radius were not responsible for the observed reduction of electrohemolysis in media containing (Gd-) DTPA (*see* Figs. 1 and 2), because it is well known that larger cells are more sensitive to electropulsing than smaller ones [8].

Effects of (Gd-) DTPA on Electrodeformation Response of RBCs to AC-Fields

The microphotographs (Fig. 3) show the electrodeformation responses of control (Fig. 3*A*) and Magnevist-treated erythrocytes (Fig. 3*C*) subjected to a 10 MHz electric field of 1.74 kV/cm at the conductivity of 1.1 mS/cm. At this field strength, the maximum steady-state deformation response to the AC field was reached within a time interval of less than 1 sec, which is in accordance with the data reported earlier [11, 28]. Upon switching off the field, both control (Fig. 3*B*) and Magnevist-treated cells (Fig. 3*D*) assumed elastically their original shape. Note that the deformation of most control cells was accompanied by the formation of a "tip" at the cell pole facing the distant electrode (Fig. 3*A*).

The deformation data from several measurements of control, Magnevist- and DTPA-treated cell samples are summarized in the histograms shown in Fig. 4. Despite the very broad populational distributions of the individual cell elongation values (coefficients of variation CV > 50%), comparison of the mean relative deformations shows that Magnevist (and DTPA) caused a significant decrease ($P < 0.001$ in both cases) in the electrodeformation response of RBCs. Magnevist and DTPA reduced the mean relative elongation from 0.52 (control) to 0.23 and 0.37, respectively (Fig. 4).

It must be noted, that the reduction of the electrodeformation response caused by (Gd-) DTPA (Figs. 3 and 4) does not necessarily mean that these compounds decreased deformability of RBCs. A possible cause for the observed behavior could also be a decrease of the cytosolic conductivity (at a fixed σ_e), because the electric stretching force at MHz frequencies and, therefore, the resulting elongation response of cells depend strongly on the conductivities of both suspending medium and cytosol (σ_e and σ_i, *see* Appendix). The external conductivity was not responsible for the observed effects of (Gd-) DTPA on cell deformation response, because all sus-

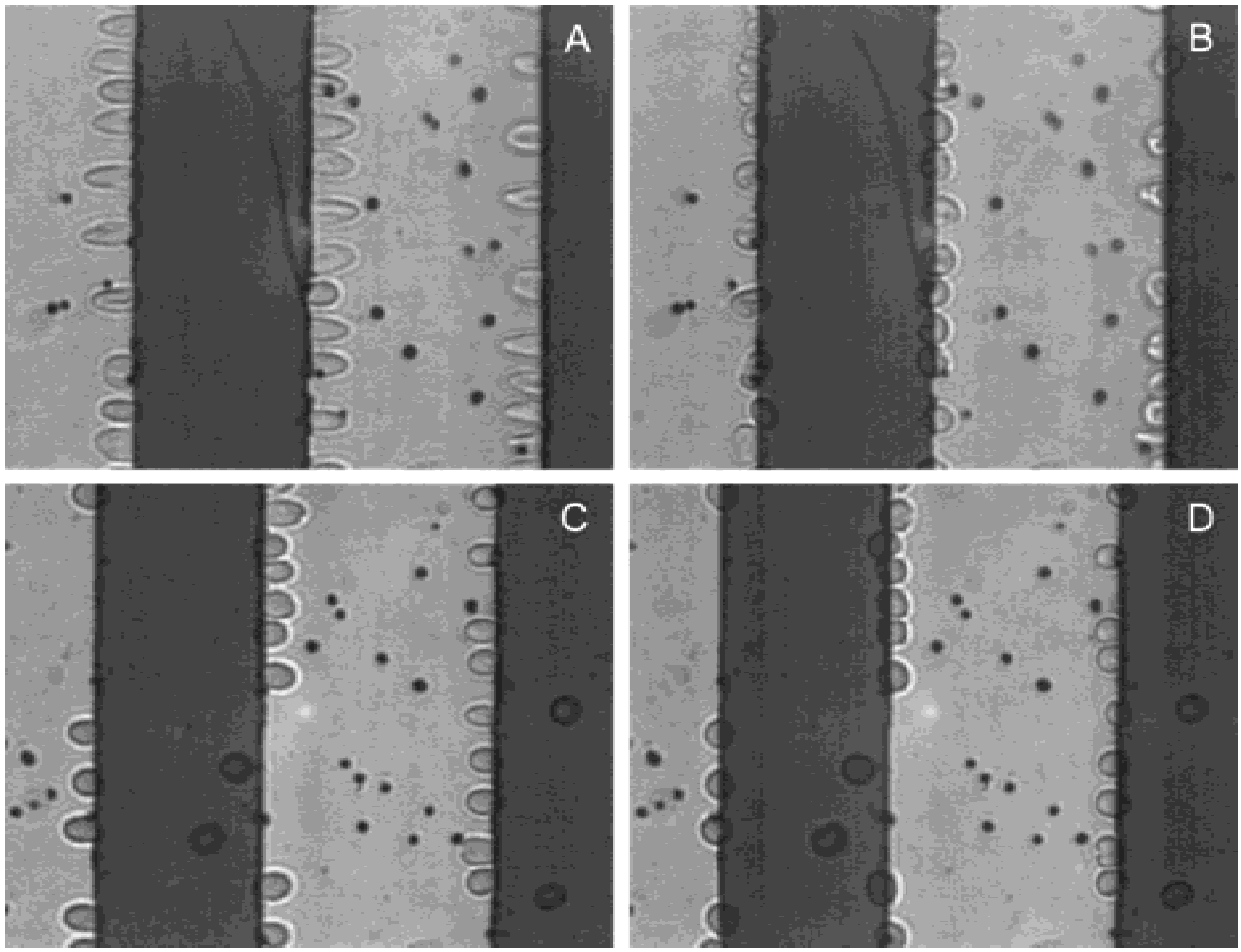

Fig. 3. Electrodeformation response of human RBCs to an AC electric field (10 MHz) of 1.74 kV/cm (*A* and *C*, elongation parallel to the field lines). The experiments were performed in isotonic media of different composition (*A* and *B:* KCl-inositol; and *C* and *D:* 10 mM Magnevist-inositol), but of the same conductivity ($\sigma_e \approx 1$ mS/cm). Upon removal of the electric field, the erythrocytes resumed elastically their original shape (*B* and *D*). Note that although the magnitudes of the electric forces acting on the cells were equal for both cell samples, the elongation of control cells (*A*) was almost twice as high as that of the erythrocytes treated with Magnevist (*C*).

pending media used in this series of deformation experiments had nearly the same conductivity of 1 mS/cm (*see* Figs. 3–6). To evaluate the electrical properties of the cytosol of RBCs suspended in control and (Gd-) DTPA containing media, measurements of electrorotation and electrodeformation spectra have been performed over a wide frequency range.

Electrodeformation and Electrorotation Spectra

Changes in the cytosolic conductivity σ_i of RBCs can be directly detected by studying their electrodeformation and electrorotation spectra, because σ_i exerts significant influence on the electromechanical responses of cells in the frequency range between 10 and 100 MHz. In addition to the σ_i value, quantitative data on the electrical properties of the plasma membrane can also be extracted from the interrelated electrodeformation and rotation spectra by using an appropriate theoretical model (*see* Appendix).

As pointed out elsewhere [43], the cellular parameters can be determined much more accurately from electrorotation than from deformation spectra, because a much broader frequency range is available for electrorotation measurements. Figure 5*B* shows the rotation spectra of control and Gd-DTPA-treated RBCs obtained at the conductivity of 1 mS/cm. The rotation spectrum of DTPA-treated erythrocytes (*data not shown*) was closely similar to that of control cells. We found that neither Magnevist nor DTPA caused any significant changes in the position of the "cytosolic" cofield rotational peak of erythrocytes: the peak frequencies f_{c2} (±SD) were 66 ± 4, 62 ± 7 and 59 ± 3 MHz for control, Magnevist and DTPA treated cells, respectively. As with the cofield peak, the low-frequency "plasma-membrane" peak was also not

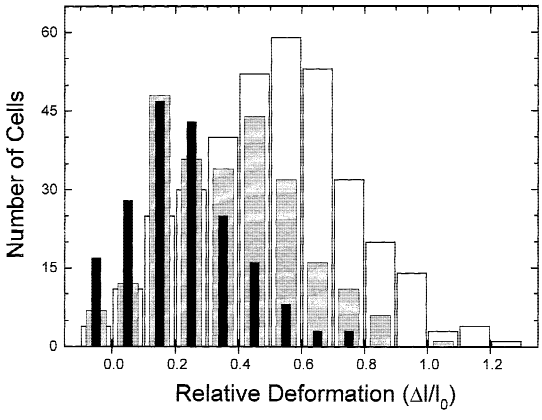

Fig. 4. Distribution of relative deformation values of erythrocytes exposed to an AC field (10 MHz) of 1.74 kV/cm: control cells (white bars; $n = 349$ cells), cells in the presence of 5 mM DTPA (gray bars; $n = 247$) and 10 mM Magnevist (black bars; $n = 190$), respectively. For each erythrocyte within the cell samples, its original length (l_0, without field) and its maximal length (l, after field application) in the direction parallel to the field lines were determined. Note that in all cell samples the electrodeformation response given by the relative cell deformation, $(l - l_0)/l_0 = \Delta l/l_0$, is subject to a large variability, i.e., the coefficients of variation (CV = SD/mean, given in percentage) are 48% (control), 58% (DTPA-) and 74% (Magnevist-treated cells). Despite this large variability, the mean $\Delta l/l_0$ values for cells treated with DTPA and Magnevist (0.37 and 0.23, respectively) are significantly lower than the value obtained on control erythrocytes ($\Delta l/l_0 = 0.52$, $P < 0.001$).

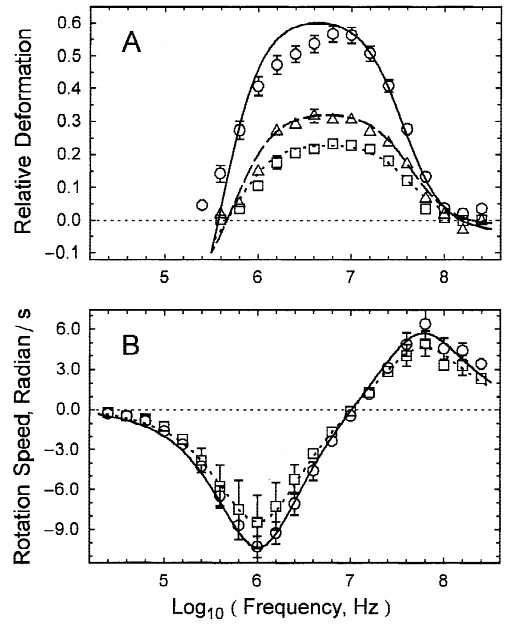

Fig. 5. Electrodeformation (*A*) and electrorotation (*B*) spectra of erythrocytes measured in isotonic media of similar conductivity (1.05 ± 0.15 mS/cm) but of different composition: control cells (circles), cells in the presence of 5 mM DTPA (triangles) and 10 mM Magnevist (squares). (*A*) In electrodeformation experiments, the cells were exposed to linear AC fields at a constant field strength of 1.74 kV/cm. The field frequency was decreased in steps from 250 MHz (5 points per decade of frequency). Each spectrum is the mean (±SE) obtained from about 70 cells in 6 independent experiments. The electrodeformation response could be measured accurately only in the frequency range of positive dielectrophoresis (about 800 kHz − 100 MHz), whereas for electrorotation experiments a much broader frequency range from about 10 kHz to 150 MHz was available (*B*). The rotation spectra are normalized to the field strength of 100 V/cm and represent the mean ± SD from at least 6 cells. The rotation spectrum of DTPA-treated cells (*not shown*) was similar to that of control cells. The various curves in *A* and *B* show best fits of the single-shell dielectric model (*see* Appendix) to the experimental points using following fitting parameters: $\varepsilon_e = 80 \cdot \varepsilon_0$, $\varepsilon_i = (70–75) \cdot \varepsilon_0$, $\sigma_e = 0.8–1.1$ mS/cm, $\sigma_i = 3–5$ mS/cm, $C_m = 0.7–1$ μF/cm^2, $G_m = 100–200$ mS/cm^2, $a = 3.3–4.5$ μm. Note that Magnevist and DTPA did not alter significantly the electrorotation behavior of RBCs, but reduced markedly the electrodeformation response of these cells.

affected by (Gd-) DTPA. A somewhat slower rotation speed in the presence of Magnevist can be explained by increased friction between the cell and glass surfaces, which might have been due to an alteration of the membrane surface charge or surface morphology [39]. The cellular electrical properties extracted from the rotation spectra by using the single-shell model are given in the legend to Fig. 5. The electrorotation measurements clearly showed that (Gd-) DTPA did not cause any significant changes in the electrical properties of erythrocytes.

This conclusion is also supported by the frequency dependences of the electrodeformation response shown in Fig. 5*A*. As with the rotation spectra, the electrodeformation spectra of control, Magnevist and DTPA treated erythrocytes could be fitted quite accurately on the basis of the single-shell model by using the electrical parameters extracted from the rotation spectra. To fit the theoretical spectra to the electrodeformation data only a scaling factor α (Appendix) for correction of cell elasticity was introduced. Taken together, the electrodeformation and rotation data (Figs. 3–5) reveal marked changes in the elastic properties of RBCs produced by DTPA and Magnevist, whereas no significant alterations of their electrical properties were found.

The fact that treatment with (Gd-) DTPA did not cause any significant changes in the electrical cell properties also means that *none* of the electrical and mechanical parameters relevant for electropermeabilization (i.e., the induced membrane voltage V_g, the time constant of membrane charging τ_m, the stretching force F_{DEF} and the time constant of the cytosol polarization τ_i, *see* Table) were affected by these compounds.

Changes in Cell Elasticity Induced by (Gd-) DTPA

To quantitate the effects of DTPA and Magnevist on the elasticity of RBCs, we studied the field-strength dependence of the elastic strains of control cells and those

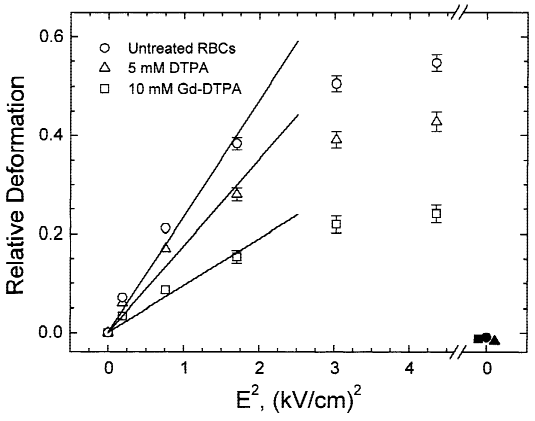

Fig. 6. Dependence of the relative cell deformation, $\Delta l/l_0$, on the quadrate of the applied field strength, E^2, at a fixed frequency of 10 MHz in media of the same conductivities (0.85 ± 0.15 mS/cm) but of different compositions (*see* Fig. 5). Each symbol represents the mean ± SE from 120–280 cells in 8–14 independent measurements. From the linear fits to the data obtained at low field strengths (<1.3 kV/cm) the mean elasticities of the RBC samples were estimated. At higher field strengths, deviations of the experimental deformation response from the theoretical function occurred in all cell samples. Upon switching off the field, the deformed cells relaxed to their original shape within about 1 sec (solid symbols).

suspended in DTPA (or Magnevist) containing media. These measurements were performed by varying the field strength from 0.2 to 2.1 kV/cm in steps of 0.2 kV/cm at a fixed frequency of 10 MHz. The conductivity of the three solutions was adjusted to the same value of 1 mS/cm. For relatively small deformations, the quadratic dependence of the electrodeformation response on the field strength predicted by the theory was observed in the three cell samples (Fig. 6). The departure from the quadratic behavior at higher field strengths was mainly due to the inhomogeneity of the field produced in the planar interdigitated microstructure used in this study.

The decreased deformation responses of cells treated with DTPA and Magnevist obviously reflect a decrease in cell elasticity. This is because under the experimental conditions used here, the electric stretching force ($F_{DEF} \propto U_{int} \cdot E^2$, where $U_{int} = (\sigma_i - \sigma_e)/(\sigma_i + 2\sigma_e)$ *see* Table) depends only on the applied field strength, whereas other parameters determining the electric force remained unchanged (σ_i, *see* above) or kept constant (σ_e). Therefore, the relative changes in cell elasticity produced by (Gd-) DTPA can be calculated from the slopes of the lines fitted to the data. For the relative deformations less than 0.2, DTPA (5 mM) and Magnevist (10 mM) reduced the elastic modulus of RBCs to about 75 and 40% of the control value, respectively.

Discussion

Red Cell Deformability

Cell deformability, which is controlled by the viscoelastic properties of the plasma membrane and membrane-attached cytoskeleton, is usually not taken into account in the studies of electropermeabilization of mammalian cells. However, this cell parameter becomes significant in view of the recent findings that the electrodeformation force on the cell membrane (caused by the electrical Maxwell stress) is responsible for the enhanced electropermeabilization of cells in low-conductivity media by both DC-pulsing [43] and AC electric fields [28]. This strongly conductivity-dependent force develops very quickly (within a few nanoseconds upon field application) due to the polarization of the highly conductive cytosol. The electric force precedes and accompanies membrane charging up to its breakdown that occurs in the microsecond range (in low-conductivity media, *see* Appendix).

There is a great body of evidence in the literature indicating that little modifications in the ionic environment (e.g., treatment with DTPA, Ca^{2+} sequestration, pH shifts, etc.) can produce dramatic changes in deformability of erythrocytes, which, in turn, is closely related to shape and mechanical stability of these cells [3, 16, 34, 38, 42]. Several experimental approaches have been developed to study red cell deformability. Thus, the average viscoelastic properties of a large number of cells can be studied using suspension methods, such as filtration [27], viscosimetry [10] and ektacytometry [29]. In contrast, experimental techniques based on the microscopic observation of individual RBCs allow the quantitative determination of cellular mechanical properties with a single-cell resolution. These techniques are: deformation using optical tweezers [6], micropipette aspiration [42], and deformation in a high frequency electric field using conventional electrodes [24, 28]. The electric fields produced within planar interdigitated microelectrodes employed in the present study provides a new method of studying the deformation response of RBCs stressed by a well-defined, unidirectional electric force. The scaling down of the electrodes allows useful fields to be imposed in more conductive (nearly physiological) media with moderate heat production, which was impossible before in the conventional electrode systems.

Effect of Chelating Agents on RBC Deformability

EDTA is widely used as anticoagulant in hemorheological and other blood related studies. As pointed out elsewhere [48], EDTA concentration in blood samples is one of the most critical parameters for rheological tests. In common with (Gd-) DTPA studied here (Figs. 3–6), EDTA has also been reported to reduce deformability of human erythrocytes, which was revealed by the conductometric microfiltration technique [27]. Our finding that Gd-DTPA reduces erythrocyte deformability also agrees with the recent observation that loading of human and rat RBCs with Magnevist (using the osmotic pulse technique) increases markedly the shear rigidity of these cells [22].

A very broad distribution of the individual cell elasticities observed in this study (Fig. 4, CV ≈ 50% for control) is in good agreement with the results obtained by means of two different microfiltration methods [5, 27]. The increased variability in the cell deformation responses after treatment with (Gd-) DTPA (Fig. 4, CV = 58–74%) suggests a high degree of heterogeneity in the sensitivity of individual cells to the chelating agents.

The molecular mechanisms underlying the observed rigidifying effect of chelating agents (EDTA, DTPA) on RBCs remain to be elucidated. It is interesting to note that other ligands (e.g., antibodies against some red cell surface markers) and calcium antagonists have also been reported to stiffen human erythrocytes [1, 7, 37]. Although EDTA does not cross the intact membrane of erythrocytes, it binds to the external membrane surface and can remove 90% of the membrane bound calcium [21]. It is also well known that many cell functions (e.g., activity of membrane enzymes, RBC shape, membrane flexibility and fusion [25, 35, 47]) are sensitively regulated by the concentration of Ca^{2+} at the cell surface and can therefore be altered by chelation of membrane calcium. Furthermore, pronounced (but reversible) changes induced by EDTA in the erythrocyte membrane morphology have been revealed by the scanning electron microscopy. Thus, after exposure to EDTA, the entire RBC surface was found to be covered with several hundreds of long, thin membrane extrusions, which, however, can be fully abolished by some di- and trivalent cations (Ca^{2+}, La^{3+}) at concentrations of about 100 μM [39]. The effects of EDTA-like compounds (mediated by Ca^{2+} sequestration) may also be due to changes in the membrane-cytoskeleton assembly which is delicately controled by the membrane surface charge, membrane lipid asymmetry and other membrane parameters [20, 25, 35].

Chelating Agents, Ca^{2+} and Electrosensitivity of Cells

The presence of small amounts (about 0.1 mM and less) of di- and trivalent cations, such as Ca^{2+}, Mg^{2+} or Zn^{2+} added to the medium, or Al^{3+} solubilized from the electrodes during field application, are beneficial for membrane stabilization of electropermeabilized cells and protoplasts [13, 32, 44]. Medium supplementation with 0.1 mM calcium acetate accelerates the resealing of the electrically permeabilized plasma membrane and improves the survival of electroporated mouse myeloma cells [9]. Divalent cations are also known to greatly reduce cell lysis caused by irreversible electric breakdown and to increase the yield of viable cell hybrids obtained by electrofusion [36, 46].

It could therefore be expected that chelating compounds, such as EDTA and its derivatives EGTA, DTPA etc., would reverse the membrane-stabilizing effect of divalent cations, i.e., render cells more sensitive to electric field exposure. In practice, however, it was found that EDTA added in 10–30 mM concentrations reduces markedly the percentage of electrohemolysis of human red blood cells and shifts the onset of hemoglobin release to higher field strengths [31, 41]. The mechanisms involving secondary osmotic effects (e.g., a field-strength dependent reflection coefficient of the cell membrane [41]) or functional alteration of transport enzymes [31] can only in part explain the observed strong protection effect of EDTA against electrohemolysis. Other parameters (e.g., red cell deformability) cannot be excluded as possible candidates because of the complexity of the breakdown event and the following secondary processes. It is also interesting to note that in about 40% of the work on electropermeabilization, the pulse media were supplemented with EDTA, EGTA and other chelating compounds despite the detrimental effects of incorporated ligands on the intracellular pH, Ca^{2+} and ATP levels (for discussion *see* [50]). In agreement with the earlier observations that EDTA suppresses electrohemolysis [31, 52], we also found that (Gd-) DTPA increased markedly the electroresistivity of human erythrocytes (Figs. 1 and 2).

The strong effects of various chelating agents on red cell deformability and electrosensitivity reported here and in the literature suggest that the increased cell stiffness might be the key parameter responsible for the electroprotection of erythrocytes by EDTA-like compounds. Further support for the deformability hypothesis comes from the observation that (Gd-) DTPA protected cells against hemolysis only if electropulsing was performed in low conductivity media (Fig. 2), that is under conditions where electrodeformation force (F_{DEF}) is operational during the electric breakdown (*see* Appendix, Table). In addition, it is possible that the red blood cell viability has also benefited from the chelator mediated membrane stiffness during the secondary stages following the membrane permeabilization by electric breakdown. Finally, the findings presented here might be of general importance for electromanipulation of cells (transfection, fusion, etc.) because cell deformability [45] as well as cell electrosensitivity [8] are reported to be cell cycle dependent.

Conclusions

We have presented evidence for a strong correlation between the ability of erythrocytes to withstand electric field exposure and the rigitity of these cells, as indicated by electropermeabilization and electrodeformation measurements using DC pulsing and high-frequency electric fields. Our results also show that relatively small alterations of membrane stiffness produced by EDTA-like ligands can lead to dramatic changes in the degree of cell membrane electropermeabilization by DC electric

pulses. This finding might have far-reaching implications for genetic manipulations of cells by electric field techniques because chemical facilitators are conceivable which modify cell deformability or alter the dependence of electrodeformation on medium conductivity. It is also evident from the present study that detailed information not only on the electrical but also on the mechanical properties of cells is essential for a better understanding and control of biophysical parameters involved in electropermeabilization (and electrofusion), and for further improvement of the present electromanipulation protocols. In addition, the results can explain many conflicting data in the literature (for review, *see* [51]) because variations of the ingredients of the pulse media (e.g., divalent cations, chelating agents etc.) may greatly influence deformability of cells and thus the uptake rate of xenomolecules as well as the release of intracellular solutes. This has to be taken into account when RBCs or lymphocytes are used as carrier systems for MR contrast agent because a reduction in deformability may lead to a rapid clearance of such manipulated cells from the blood circulation. Strategies to overcome the DTPA-induced deformability changes would be the replacement of this chelating agent by other ligands (e.g., albumin) or by incorporation of compounds into the membrane of the Gd-DTPA-treated RBCs or lymphocytes which compensate the diminished deformability of the cells.

The authors thank Elfriede Reisberg (Julius-von-Sachs-Institut für Biowissenschaften, Universität Würzburg) for the ICP measurements. This work was supported by a grant of the DFG (Zi-99/11-1) to U.Z.

References

1. Abe, H., Katada, K., Orita, M., Nishikibe, M. 1991. Effects of calcium antagonists on the erythrocyte membrane. *J. Pharm. Pharmacol.* **43:**22–26
2. Arnold, W.M., Zimmermann, U. 1982. Rotating field induced rotation and measurement of the membrane capacitance of single mesophyll cells of *Avena sativa*. *Z. Naturforsch.* **37c:**908–915
3. Bakaltcheva, I., Rudolph, A.S., Spargo, B.J. 1997. Shape stabilizing agents protect erythrocytes against freeze-thaw damage. *Cryo-Lett.* **18:**165–178
4. Brasch, R.C. 1992. New directions in the development of MR imaging contrast media. *Radiology* **183:**1–11
5. Brody, J.P., Han, Y., Austin, R.H., Bitensky, M. 1995. Deformation and flow of red blood cells in a synthetic lattice: Evidence for an active cytoskeleton. *Biophys. J.* **68:**2224–2232
6. Bronkhorst, P.J.H., Streekstra, G.J., Grimbergen, J., Nijhof, E.J., Sixma, J.J., Brakenhoff, G.J. 1995. A new method to study shape recovery of red blood cells using multiple optical trapping. *Biophys. J.* **69:**1666–1673
7. Chasis, J.A., Schrier, S.L. 1989. Membrane deformability and the capacity for shape change in the erythrocyte. *Blood* **74:**2562–2568
8. Djuzenova, C.S., Sukhorukov, V.L., Klöck, G., Arnold, W.M., Zimmermann, U. 1994. Effect of electric field pulses on the viability and on the membrane-bound immunoglobulins of LPS-activated murine B-lymphocytes: correlation with the cell cycle. *Cytometry* **15:**35–45
9. Djuzenova, C.S., Zimmermann, U., Frank, H., Sukhorukov, V.L., Richter, E., Fuhr, G. 1996. Effect of medium conductivity and composition on the uptake of propidium iodide into electropermeabilized myeloma cells. *Biochim. Biophys. Acta* **1284:**143–152
10. Dumas, D., Gouin, F., Viriot, M.-L., Stoltz, J.-F. 1997. Effect of glutaraldehyde on hemoglobin-dependent quenching of pyrene fluoreschence. Application to oxygen diffusion in erythrocyte. *Clin. Hemorheol. Microcircul.* **17:**291–297
11. Engelhardt, H., Sackmann, E. 1988. On the measurement of shear elastic moduli and viscosities of erythrocyte plasma membranes by transient deformation in high frequency electric fields. *Biophys. J.* **54:**495–508
12. Felix, R., Heshiki, A., Hosten, N., Hricak, H. 1998. Magnevist: Monograph. Blackwell Wissenschafts-Verlag, Berlin
13. Friedrich, U., Stachowicz, N., Simm, A., Fuhr, G., Lucas, K., Zimmermann, U. 1998. High efficiency electrotransfection with aluminum electrodes using microsecond controlled pulses. *Bioelectrochem. Bioenerg.* **47:**103–111
14. Fuhr, G., Zimmermann, U., Shirley, S.G. 1996. Cell motion in time-varying fields: Principles and potential. *In:* Electromanipulation of Cells. U. Zimmermann and G.A. Neil, editors. pp. 259–328. CRC Press, Boca Raton, FL
15. Gennaro, M.C., Aime, S., Santucci, E., Causa, M., De Stefano, C. 1990. Complexes of diethylenetriaminepentaacetic acid as contrast agents in NMR imaging computer simulation of equilibria in human blood plasma. *Anal. Chim. Acta* **233:**85–100
16. Gimsa, J. 1998. A possible molecular mechanism governing human erythrocyte shape. *Biophys. J.* **568:**568–569
17. Gimsa, J., Marszalek, P., Loewe, U., Tsong, T.Y. 1991. Dielectrophoresis and electrorotation of neurospora slime and murine myeloma cells. *Biophys. J.* **60:**749–760
18. Gimsa, J., Müller, T., Schnelle, T., Fuhr, G. 1996. Dielectric spectroscopie of single human erythrocytes at physiological ionic strength: dispersion of the cytoplasm. *Biophys. J.* **71:**495–506
19. Glaser, R. 1982. Echinocyte formation induced by potential changes of human red blood cells. *J. Membrane Biol.* **66:**79–85
20. Godin, C., Caprani, A. 1997. Effect of blood storage on erythrocyte/wall interactions: Implications for surface charge and rigidity. *Eur. Biophys. J.* **26:**175–182
21. Harrison, D.G., Long, C. 1968. The calcium content of human erythrocytes. *J. Physiol.* **199:**367–381
22. Johnson, K.M., Tao, J.Z., Kennan, R.P., Gore, J.C. 1998. Gadolinium-bearing red cells as blood pool MPI contrast agents. *Magnet. Res. Med.* **40:**133–142
23. Jones, T.B. 1995. Electromechanics of Particles, Cambridge University Press, New York
24. Kage, H.S., Engelhardt, H., Sackmann, E. 1990. A precision method to measure average viscoelastic parameters of erythrocyte populations. *Biorheology* **27:**67–78
25. Kahana, E., Streichman, S., Silver, B. 1991. The role of electrostatic forces in the interaction between the membrane and cytoskeleton of human erythrocytes. *Biochim. Biophys. Acta* **1066:**1–5
26. Kinosita, K., Tsong, T.Y. 1977. Hemolysis of human erythrocytes by a transient electric field. *Proc. Natl. Acad. Sci. USA* **74:**1923–1927
27. Koutsouris, D., Guillet, R., Wenby, R.B., Meiselman, H.J. 1989. Determination of erythrocyte transit times through micropores: II) Influence of experimental and physiological factors. *Biorheology* **26:**881–898
28. Krueger, M., Thom, F. 1997. Deformability and stability of erythrocytes in high-frequency electric fields down to subzero temperatures. *Biophys. J.* **73:**2653–2666
29. Labow, R.S., Card, R.T., Rock, G. 1987. The effect of the plasti-

cizer di(2-ethylhexyl)phthalate on red cell deformability. *Blood* **70:**319–323
30. Lynch, P.T., Davey, M.R. 1996. Electrical Manipulation of Cells. Chapman & Hall, New York
31. Nanda, G.S., Mishra, K.P. 1994. Modification of electroporative response of erythrocytes by EDTA in isotonic solutions. *Bioelectrochem. Bioenerg.* **34:**189–193
32. Neil, G.A., Zimmermann, U. 1993. Electroinjection. *Meth. Enzymol.* **221:**339–361
33. Neumann, M., Lerche, D., Meier, W., Paulitschke, M. 1993. Bewertung der Ganzzelldeformierbarkeit einzelner Erythrozyten mittels Kapillar-Rigidometer–Möglichkeiten zur Standardisierung und Relativierung. *Biomed. Technik* **38:**204–212
34. Noji, S., Taniguchi, S., Kon, H. 1987. Spin label study of erythrocyte deformability: Ca^{2+}-Induced loss of deformability and the effects of stomatocytogenic reagents on the deformability loss in human erythrocytes in shear flow. *Biophys. J.* **52:**221–227
35. Ohki, S., Arnold, K. 1990. Surface dielectric constant, surface hydrophobicity and membrane fusion. *J. Membrane Biol.* **114:** 195–203
36. Ohno-Shosaku, T., Okada, Y. 1985. Electric pulse-induced fusion of mouse lymphoma cells: Roles of divalent cations and membrane liquid domains. *J. membrane Biol.* **85:**269–280
37. Paulitschke, M., Nash, G.B., Anstee, D.J., Tanner, M.J., Gratzer, W.B. 1995. Perturbation of red blood cell membrane rigidity by extracellular ligands. *Blood* **86:**342–348
38. Peters, S.M.A., de Jong, M.D., Bindels, R.J.M., van Os, C.H., Wetzels, J.F.M. 1998. Effects of renal cytoprotective agents on erythrocyte membrane stability. *Life Sci.* **63:**975–983
39. Pinteric, L., Manery, J.F., Chaudry, H., Madapallimattam, G. 1975. The effect of EDTA, cations, and various buffers on the morphology of erythrocyte membrane: An electron-microscopic study. *Blood* **45:**709–724
40. Schmiedl, U., Moseley, M.E., Ogan, M.D., Chew, W.M., Brasch, R.C. 1987. Comparison of initial biodistribution patterns of Gd-DTPA and albumin-(Gd-DTPA) using rapid spin-echo MR imaging. *J. Comput. Assist. Tomogr.* **11:**306–313
41. Schneeweiss, F., Zimmermann, U., Saleemuddin, M. 1977. Preparation of uniform haemoglobin free human erythrocyte ghosts in isotonic solution. *Biochim. Biophys. Acta* **466:**373–378
42. Smith, B.D., La Celle, P.L. 1979. Parallel decrease of erythrocyte membrane deformability and spectrin solubility at low pH. *Blood* **53:**15–18
43. Sukhorukov, V.L., Mussauer, H., Zimmermann, U. 1998. The effect of electrical deformation forces on the electropermeabilization of erythrocyte membranes in low- and high-conductivity media. *J. Membrane Biol.* **163:**235–245
44. Tomov, T.C., Tsoneva, I.C., Doncheva, J.C. 1988. Electrical stability of erythrocytes in the presence of divalent cations. *Biosci. Rep.* **8:**421–426
45. Tsai, M.A., Waugh, R.E., Keng, P.C. 1996. Cell-cycle dependence of HL-60 cell deformability. *Biophys. J.* **70:**2023–2029
46. Vienken, J., Zimmermann, U. 1985. An improved electrofusion technique for production of mouse hybridoma cells. *FEBS Lett.* **182:**278–280
47. Wiley, J.S., McCulloch, K.E. 1982. Calcium ions, drug action and the red cell membrane. *Pharmacol. Ther.* **18:**271–292
48. Zhu, J.-C., Stone, P.C.W., Stuart, J. 1989. Measurement of erythrocyte deformability by cell transit analyser. *Clin. Hemorheol.* **9:**897–908
49. Zimmermann, U. 1983. Cellular drug-carrier systems and their possible targeting. *In:* Targeted Drugs. E. Goldberg, editor. pp. 153–199. John Wiley, New York
50. Zimmermann, U. 1996. The Effect of High Intensity Electric Field Pulses on Eukaryotic Cell Membranes: Fundamentals and Applications. *In:* Electromanipulation of Cells. U. Zimmermann and G.A. Neil, editors. pp. 1–106. CRC Press, Boca Raton, FL
51. Zimmermann, U., Neil, G.A. 1996. Electromanipulation of Cells, CRC Press, Boca Raton, FL
52. Zimmermann, U., Pilwat, G., Holzapfel, C., Rosenheck, K. 1976. Electrical hemolysis of human and bovine red blood cells. *J. Membrane Biol.* **30:**135–152

Appendix

An electric field E (alternating, rotating or DC pulsing) imposed on a freely suspended cell induces a dipole moment μ within the cell and also charges the plasma membrane [14, 18, 23, 50]. The induced dipole μ and the voltage drop V_g across the plasma membrane arise from the charges that accumulate at the two membrane interfaces. Due to the layered structure of the cell, its dipole moment depends on time or field frequency in a quite complicated manner (Figs. A1 and A2). The electrostatic interaction of the cell dipole μ with the applied field results in a variety of electromechanical phenomena (e.g., electrorotation, ROT [2], and electrodeformation, DEF [43], etc.), whereas the induced voltage V_g can lead to membrane permeabilization via the electric breakdown mechanism if V_g exceeds 1 V [50].

For modelling the frequency spectra of V_g, DEF and ROT, the erythrocyte is usually viewed as a conductive sphere (the cytoplasm) with radius a, conductivity σ_i, and permittivity ε_i, which is covered by a layer (the plasma membrane) of thickness $d << a$, conductivity $\sigma_m << \sigma_i$, permittivity ε_m, and area-specific conductance $G_m = \sigma_m/d$ and capacitance $C_m = \varepsilon_m/d$. The cell is suspended in an aqueous medium with permittivity $\varepsilon_e = 80 \cdot \varepsilon_0$ and conductivity σ_e. In alternating or rotating electric fields (the frequency domain), the dipole is a function of the complex cell polarizability, which is described by the frequency-dependent Clausius-Mosotti function U^*: $\mu = 4\pi \cdot a^3 \cdot \varepsilon_e \cdot E \cdot U^*$ (*see* Table). The DEF and ROT responses are proportional to the real and imaginary parts of the Clausius-Mosotti function, respectively. For relatively small cell deformations, the following relation holds between the elastic strain ($\Delta l/l_0$), E and U^* [43]:

$$\frac{\Delta l}{l_0} \propto \alpha \cdot E^2 \cdot Re(U^*) \tag{1}$$

where the scaling factor α accounts for the elastic cell properties. Positive and negative values of the strain (i.e., of Re(U^*)) indicate cell elongation and compression, respectively.

In a rotating field, the steady state electroroation speed (Ω) of a cell suspended in a medium of viscosity η is given by [14, 17, 23]:

$$\Omega = -\frac{\varepsilon_e \varepsilon_0 E^2}{2\eta} Im(U^*) \tag{2}$$

Fig. A1 *A* and *C* compares the frequency spectra of the three parameters V_g, DEF and ROT at two different conductivities of the medium. The two rotational peaks with the characteristic frequencies f_{c2} (polarization of the cytoplasm) and f_{c1} (plasma membrane charging) and the corresponding dispersions in the DEF and V_g spectra are caused by two Maxwell-Wagner relaxation effects at the inner and outer boundaries of the plasma membrane, respectively. Note that maximum membrane charging (V_g) is achieved only in the low frequency range ($f < f_{c1}$) and both dispersions move toward higher frequencies with increasing medium conductivity (for numeric values of f_{c1} and f_{c2} *see* Table). Note, that the field strength of 1 kV/cm assumed for these calculations is not sufficient to induce the critical membrane voltage of 1 V. There are three frequency regions where ROT is negligible and, therefore, sim-

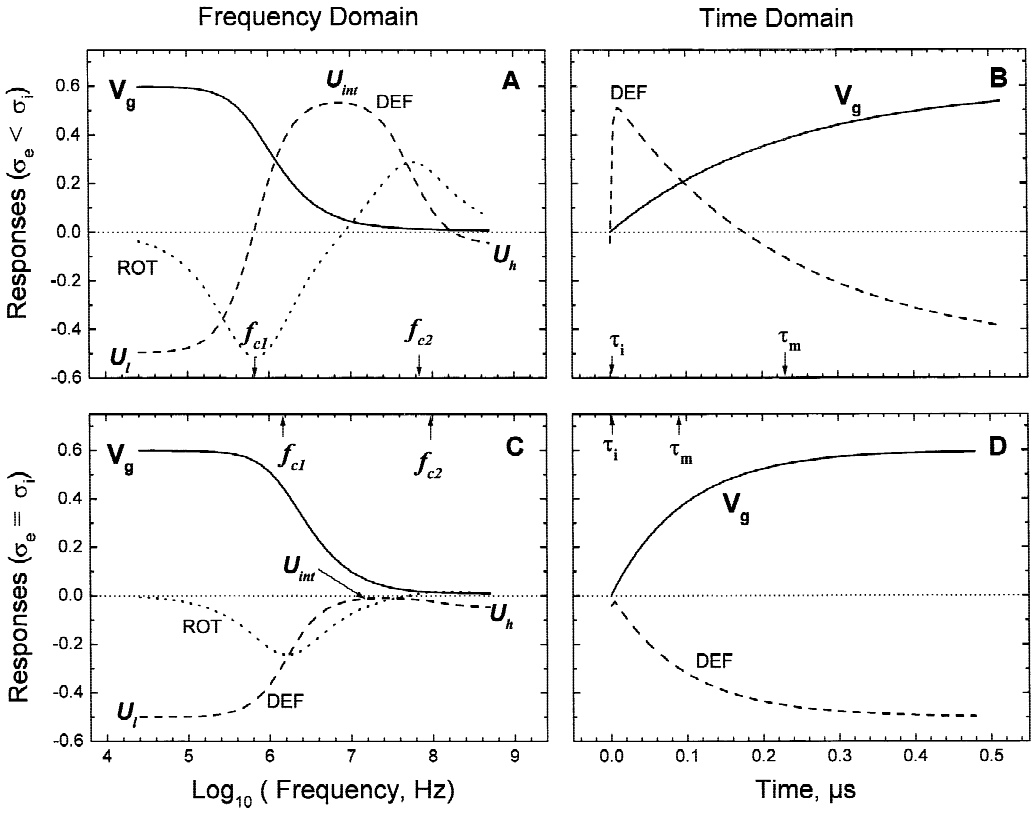

Fig. A1. Theoretical, frequency and time domain plots of the induced membrane potential (V_g, solid lines), deformation force (DEF, dashed lines) and cell rotation (ROT, dotted lines) in low (*A* and *B*, σ_e = 1 mS/cm) and highly (*C* and *D*, σ_e = 5 mS/cm) conductive media. The cell is approximated by the single-shell model with the following parameters: a = 4 µm, C_m = 0.8 µ*F*/cm^2, G_m = 10 mS/cm^2, ε_i = 70 ε_0, σ_i = 5 mS/cm, ε_e = 80 ε_0. The applied field strength was assumed to be 1 kV/cm. In the frequency domain (*A* and *C*), the electrodeformation and rotation responses are represented by the real and imaginary parts of the cell polarizability *U**, respectively. The curves in the time domain (*B* and *D*, response to a step-function electric field) were calculated from the frequency spectra (*A* and *C*) using standard transformation methods. The time constant of membrane charging τ_m is related to f_{c1} as: $\tau_m = (2 \cdot \pi \cdot f_{c1})^{-1}$ (*see* Table), where f_{c1} is the characteristic frequency of antifield rotation. The time constant of the cytosolic polarization is given by $\tau_i = (2 \cdot \pi \cdot f_{c2})^{-1}$, where f_{c2} is the characteristic frequency of cofield rotation. The parameters U_1, U_{int} and U_h represent the effective cell polarizabilities at very low, intermediate and very high frequencies, respectively. For further explanations, *see* text.

plified expressions for the polarizability *U** can be derived for the low, intermediate and high frequency ranges (U_l, U_{int} and U_h, Table). DEF is independent of σ_e at high frequencies ($U_h \approx -0.04$) and low frequencies ($U_l \approx -0.5$, compression), but it depends strongly on σ_e at intermediate frequencies (U_{int}). Within this frequency range, cell stretching (positive values of U_{int}) occurs only in low-conductivity media (Fig. A1*A*, $\sigma_e < \sigma_i$), whereas at higher conductivities, $\sigma_e \geq \sigma_i$, the stretching force vanishes (Fig. A1*C*).

The induced interfacial charges, the corresponding dipole moment, µ, and the resulting deformation forces, F_d, are illustrated in Fig. A2. The field distribution around a model cell, calculated for two conductivities and three frequency regions (for details *see* [43]), are also shown. In the low frequency range, the induced dipole moment µ is anti-parallel to the field *E*, resulting in compression, and nearly independent of σ_e (Fig. A2*A*). At intermediate frequencies, the conductivities of cytosol and suspending medium are the main determinants of the resulting deformation responses (U_{int}, Table). For $\sigma_e < \sigma_i$, the induced dipole is parallel to the external field, resulting in elongation (Fig. A2*B*). For $\sigma_e = \sigma_i$, no deformation forces appear (Fig. A2*D*). In the high frequency range, the dipole (U_h) is negligible and independent of conductivities (Fig. A2*C*).

In response to an applied DC electric field, V_g grows monoexponentially with time (Table, Fig. A1*B* and *D* solid lines). In contrast, the temporal polarization response of cells µ(*t*), given by DEF = *U*(*t*), is more complex, as shown in Fig. A1*B* and *D* (dashed lines) for two different external conductivities. After application of a DC-field pulse, the magnitude and the direction of the induced dipole moment µ is given first by U_h, then by U_{int} and finally by U_l. Note that under low conductivity conditions, the dipole µ changes twice its sign as a function of time (Fig. A1*B*, dashed line), which means that transitions from cell compression to cell elongation force occur upon field application. It is obvious that in the case of $\sigma_e < \sigma_i$ (dashed curve in Fig. A1*B*) the elongation force reaches its maximum value about 1 nsec after pulse administration, which is much faster than the charging process of the membrane given by V_g (τ_m = 0.23 µsec). If $\sigma_e \approx \sigma_i$, the elongation force does not appear (dashed curve in Fig. A1*D*). Calculations show that the field strength of 4 kV/cm, as used in the electrohemolysis experiments, will induce breakdown of the membrane 42 nsec (σ_e = 1 mS/cm) or 18 nsec (σ_e = 5 mS/cm) after the field pulse application. This means that electric breakdown of the cell membrane occurs within the time scale where the transient stretching force is operational. The response to this transient force has

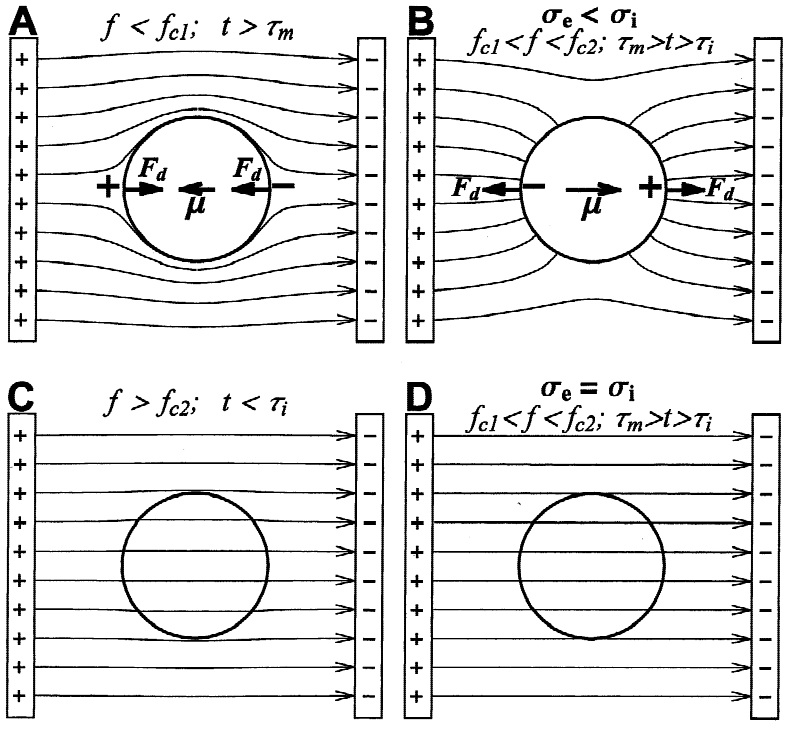

Fig. A2. The diagrams show the electric field distributions, the induced interfacial charges, the corresponding induced-dipole moments, μ, and the deformation forces, F_d, acting on a spherical cell exposed to homogeneous AC fields of various frequencies and conductivities. The field lines (arrows) and the dipole moments were calculated as described elsewhere [43], for a cell suspended in *low* and *high-conductivity* solutions ($\sigma_e < \sigma_i$ and $\sigma_e \approx \sigma_i$, respectively). In the low-frequency region (*A*), the induced dipole, μ, is oriented in the direction opposite to the field for both cases, i.e., $\sigma_e < \sigma_i$ and $\sigma_e \approx \sigma_i$. Note that μ is proportional to $U_1 = -0.5$. At the intermediate frequencies the dipole ($\mu \propto U_{int}$) is large and it is oriented in the direction of the field if $\sigma_e < \sigma_i$ (*B*). In contrast, if $\sigma_e \approx \sigma_i$ (*D*) the dipole in the MHz range becomes negligible. In the high-frequency range (*C*), the induced dipole ($\mu \propto U_h$) is also negligible, because ε_i is close to ε_e. Note that the interaction of the local electric field with the induced charges leads to the occurrence of deformation forces (F_d). For further explanation, *see* text.

to be distinguished from the steady-state deformation of erythrocytes upon application of a *constant* force. The time constant of RBC elongation in response to a constant force is of the order of 0.1–1 sec [11, 28].

It was pointed out elsewhere [43] that (i) transient electrodeformation force (elongation/compression) precedes and accompanies membrane charging in response to pulsed DC electric field and that (ii) under conditions which leads to cell elongation (that is $\sigma_e < \sigma_i$, Fig. A1*B*) the transient stretching force can affect the enlargement of the electroleaks generated via electric breakdown at the membrane sites oriented in field direction. This transient stretching force on the cell membrane might be responsible for the enhanced electropermeabilization of mammalian cells under low conductivity conditions reported here (Fig. 2) and in the literature [9, 26, 43].